International Symposium
On Turbulence and Shear Flow
Phenomena (TSFP-9)
June 30 - July 3, 2015 *Melbourne, Australia*

SMALL-SCALE PHASE ORGANIZATION THROUGH LARGE-SCALE INPUTS IN A TURBULENT BOUNDARY LAYER

Subrahmanyam Duvvuri[†] **& Beverley J. McKeon**
Graduate Aerospace Laboratories
California Institute of Technology
Pasadena, CA 91125, USA
[†]subrahmanyam@caltech.edu

ABSTRACT

A synthetic large-scale motion is excited in a flat plate turbulent boundary layer experiment and its influence on small-scale turbulence is studied. The synthetic scale is seen to alter the average natural phase relationships in a quasi-deterministic manner, and exhibit a phase-organizing influence on the directly coupled small-scales. The results and analysis presented here are of interest from a scientific perspective, and also suggest the possibility of engineering schemes for favorable manipulation of energetic small-scale turbulence through practical large-scale inputs.

BACKGROUND AND INTRODUCTION

Phase relationships in turbulent shear flows have been an area of research interest since the pioneering works of Brown & Thomas (1977) and Bandyopadhyay & Hussain (1984) on the correlations between large and small scales. This area has seen a recent surge in activity with several investigations, experimental and numerical, over the past two decades confirming the presence of very-large-scale motions (VLSM) in wall-bounded turbulent flows (see Smits *et al.* 2011 and reference therein). Of particular interest, from a scientific and an engineering perspective, is the influence of large scales on small-scale turbulence through nonlinear coupling. The experimental study of Rao *et al.* (1971) showing the outer scaling of turbulent bursts in the inner region of a boundary layer provided the first clear evidence of such scale coupling, and emphasized the significance of inner-outer interactions in wall turbulence.

More recently, through a careful analysis of high-Reynolds number boundary layer data, Hutchins & Marusic (2007) suggested an amplitude modulation influence on near-wall small-scale turbulence by large-scale motions centered in the log region. The modulation effect was later quantified by Mathis *et al.* (2009) through a demodulation scheme in which a correlation coefficient (termed amplitude modulation coefficient R) between the large-scale velocity signal and an envelope of the small-scale velocity signal from a turbulent boundary layer was taken to be a measure of amplitude modulation. Jacobi & McKeon (2013) using a co-spectral technique demonstrated that the strongest modulating influence in the large-scale signal comes from a wavenumber that matches the VLSM. Mathis *et al.* (2009) also noted an interesting similarity between the behavior of the amplitude modulation coefficient and skewness (S) of the turbulence signal with wall-normal distance. Schlatter & Örlu (2010) suggested that the amplitude modulation coefficient is to a large extent another representation of a cross term in the scale-decomposed skewness factor. A clear connection was established empirically by Mathis *et al.* (2011) between the cross term $3u_L u_S^2$ of the skewness, obtained by a scale-decomposition of the velocity signal u into large- and small-scale components ($u = u_L + u_S$), and the amplitude modulation coefficient across a range of Reynolds numbers in a turbulent boundary layer. Bernardini & Pirozzoli (2011) studied two-point velocity correlations obtained from DNS data of a compressible turbulent boundary layer to show clear evidence of top-down influence of large-scale outer events on the small-scales in the inner part of the boundary layer, and the same was interpreted as amplitude modulation. Chung & McKeon (2010) note that the amplitude modulation coefficient can also be interpreted as a phase relationship between the large scales and the small-scale envelope. It is clear from the correlation studies thus far that a definitive phase relationship exists between large- and small-scale activity in wall-bounded turbulent flows.

A formal relationship between the amplitude modulation coefficient and the skewness for a general statistically stationary signal was established recently by the authors (Duvvuri & McKeon 2015, henceforth referred to as DM15) through a simple multi-scale analysis. Both the quantities were shown to be fundamentally a measure of phase in interactions between triadically consistent scales, *i.e.* sets of wavenumbers $\{k_l, k_m, k_n\}$ such that $k_l = k_n - k_m$. Note that triadic interactions assume physical significance given the quadratic nature of non-linearity that governs coupling between scales. More interestingly, DM15 describes an experiment in which a synthetic large-scale motion was excited in a turbulent boundary layer to generalize and study the influence of large-scale motions on small-scale turbulence. It was shown that the naturally existing phase relationships in the flow can be manipulated in a quasi-deterministic manner. The influence of the synthetic scale is felt strongly by directly coupled pairs of small-scale wavenumbers; a clear phase-organization is seen among the triadically coupled small-scales.

In this paper we briefly recount details of the DM15 experiment and multi-scale analysis, and expand upon aspects not dealt with at length previously. In particular, we show here in detail the formulation of the amplitude weighted triadic small-scale envelope and demonstrate the small-scale phase-organization. A connection is then made between the triadic envelope and the oscillatory component of the

normal streamwise Reynolds stress, and finally, efforts to model and explain the experimentally observed phase behavior of the same are very briefly discussed.

SYNTHETIC LARGE-SCALE MOTION

Jacobi & McKeon (2011) performed a systematic study of a spatially-impulsive k-type wall roughness element in a turbulent boundary layer and demonstrated its effectiveness in exciting a spatio-temporal mode (or a traveling wave) in the flow. The same technique is used here with modifications to minimize static roughness effects and focus on the dynamic forcing of a single spatial (streamwise direction) and temporal scale. The experimental description below can be found in greater detail in DM15 and in Duvvuri & McKeon (2014), henceforth referred to as DM14.

Experimental Set-up

A flat plate zero-pressure-gradient boundary layer flow was perturbed (or forced) by a spatially-impulsive patch of dynamic roughness; the flow has a free-stream velocity $U_\infty = 22.1$ m/s and is fully turbulent at the perturbation location with momentum thickness based Reynolds number $Re_\theta \approx 2750$ (see figure 1). The roughness element consists of a thin straight rib at the wall aligned along spanwise direction, and oscillated sinusoidally in the wall-normal direction (y) at a set frequency f = 50 Hz to force a single spanwise constant (2D) spatio-temporal mode in the downstream boundary layer. The temporal wavenumber ω (= $2\pi f$) is set by the forcing frequency and the spatial (streamwise direction x) wavenumber is dependent on the roughness geometry; it is determined *a posteriori* from experimental data as explained shortly. Phase-locked hot wire measurements were made at three different downstream locations of the perturbation as marked in figure 1; data presented in this paper is from the first measurement station (referred to as station-1) located at $x = 2.7\delta$ downstream of the roughness perturbation ($\delta = 16.55$ mm is the local boundary layer thickness). At this location $Re_\theta = 2780$ and the friction Reynolds number is estimated using the Coles-Fernholz empirical relation to be $Re_\tau \approx 940$.

Turbulence Spectrum

The time-resolved hot wire velocity signal $U(y,t)$, where t is time, is decomposed into mean $\overline{U}(y)$ and fluctuating components $u(y,t)$ (Reynolds decomposition). Figure 2 shows the power spectrum of the fluctuations (E_{uu}) for the forced flow in a pre-multiplied form, and also the difference spectra showing the fractional change in power levels between forced and canonical flows $\left(E^F_{uu} - E^C_{uu}\right)$ relative to the canonical flow $\left(E^C_{uu}\right)$ with no forcing. Note here that temporal data is projected onto the streamwise direction at all wall-normal locations using the local mean velocity $\overline{U}(y)$. The energetic narrow-band activity extending in the wall-normal direction in the large-scale region of the spectrum shows the presence of a synthetic scale, and this is confirmed by the difference spectrum. The cut-off filter to separate large and small scales for subsequent analysis is set at $\lambda_\gamma = 5\delta$, where the separation between the synthetic large scale and energetic small scales is clear for all y.

It is important to note that multiple scales are excited immediately downstream of the roughness perturbation ($x \lesssim 1$). However, these evanescent modes decay quickly and the flow is dominated by a single spatio-temporal mode for a relatively large streamwise extent. As the forcing is spatially-impulsive and applied only at one location, the synthetic mode gradually decays with downstream distance (see figure 2 of DM14).

The Synthetic Large Scale

Following Hussain & Reynolds (1970), the turbulent fluctuations are further decomposed as $u(y,t) = \widetilde{u}(y) + u'(y,t)$ into coherent and turbulent parts, here $\widetilde{u}$ is the periodic velocity component associated with the forcing and u' is rest of the turbulence. $\widetilde{u}(y)$ is obtained by subjecting $u(y,t)$ to a narrow-band-pass filter around the forcing frequency and then phase-averaging the filter output with respect to the input forcing signal (see DM14 for details); it represents the amplitude and shape of the synthetic mode. Figure 3 shows $\widetilde{u}(y)$ at station-1 ($x = 2.7\delta$) over one temporal period; $\widetilde{u}(y)$ is also calculated at $x = 3.6\delta$ and $x = 5.4\delta$ (not shown here).

The streamwise wavenumber k_{sls} for the mode is estimated by tracking the change in phase of $\widetilde{u}$ with x (between successive measurement stations) at its wall-normal peak amplitude location. The phase value is picked from the peak location as it suffers the least from de-correlating effects from nearby spectral content during the phase-averaging procedure. From the change in phase of $\widetilde{u}$ between the first two measurement stations (where the synthetic mode activity is the strongest), k_{sls} is estimated to be $0.42\delta^{-1}$ ($\lambda_{sls} = 15\delta$). The mode velocity is then $c = \omega/k_{sls} = 0.59U_\infty$, and it's critical layer location y_c where $c = \overline{U}(y_c)$ is estimated using the mean velocity profile to be 0.072δ ($y_c^+ \approx 68$). While this estimate of y_c is fairly good, as judged by its proximity to the wall-normal peak in $\widetilde{u}$, it is important to note its sensitivity to k_{sls} due to the sharp mean velocity gradient in the near-wall region. A slight uncertainty in the estimation of k_{sls} (and hence c), possibly due to the finite number of phase-averaging cycles, can result in a significant change to y_c. In the following section we show the influence of the synthetic large scale on the natural triadic phase relationships in a turbulent boundary layer.

TRIADIC SCALE INTERACTIONS

An understanding of the triadic interactions between scales of turbulence provides valuable insight into the complex dynamics of turbulent flows. For instance, Sharma & McKeon (2013) show through analysis of the Navier-Stokes resolvent operator that a set of three triadically consistent spatio-temporal modes is able to produce complex structures such as modulating packets of hairpin vortices observed in wall-bounded turbulent flows. We summarize here the analysis of DM15 showing skewness and amplitude modulation coefficient to be measures of phase in triadic interactions.

Consider a signal u of statistically stationary velocity fluctuations in streamwise direction x

$$u = \sum_{i=1}^{\infty} \alpha_i \sin(k_i x + \phi_i), \tag{1}$$

with $0 < k_i < k_j$ for $i < j$ and k_1 being the largest scale in the signal. The skewness $S = \langle u^3 \rangle / \sigma^3$, where $\langle\ \rangle$ denotes the mean operator and σ is the standard deviation of u, can

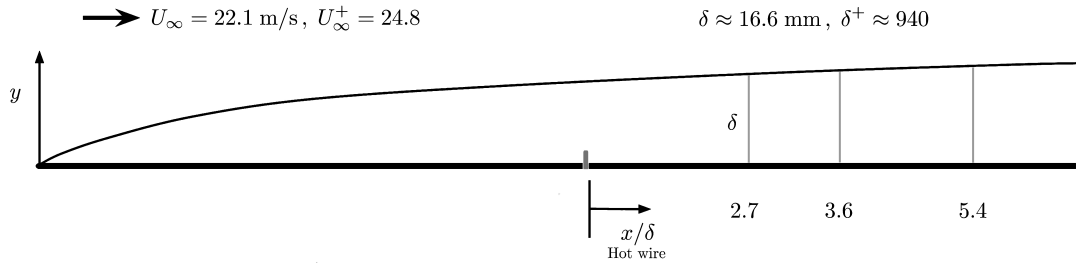

Figure 1. Schematic of the experimental set-up (not to scale). The turbulent boundary layer is forced by a spatially impulsive single rib dynamic roughness at a streamwise location ($x = 0$) where the momentum thickness Reynolds number $Re_\theta \approx 2750$. The rib has a height of 0.76 mm (oscillation amplitude) and a width (streamwise extent) of 1.5 mm. Phase-locked hot wire measurements are made at three downstream stations as marked.

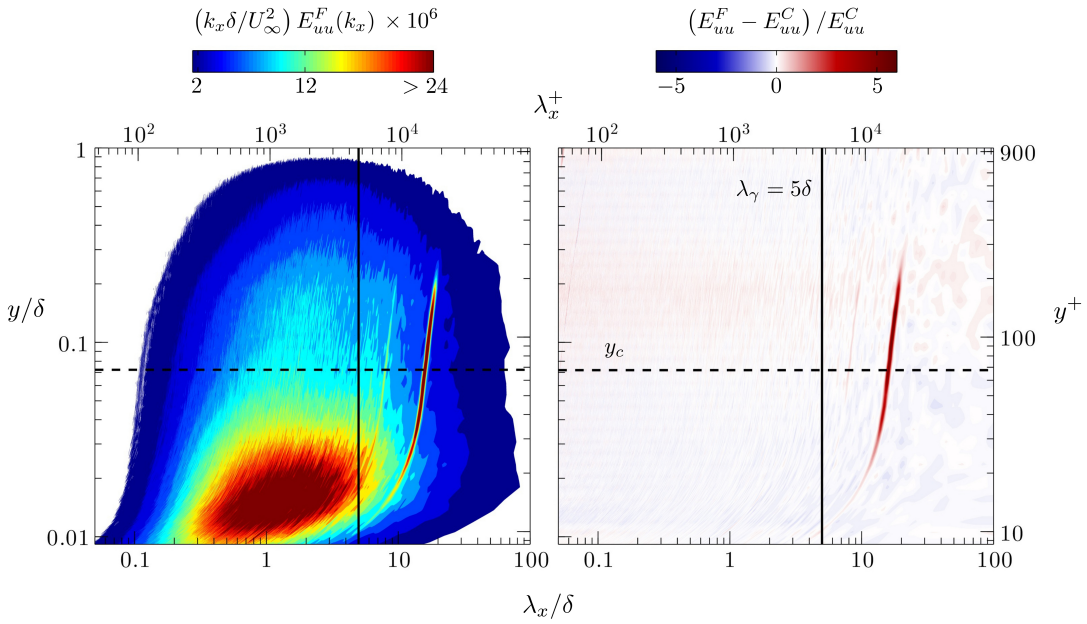

Figure 2. Pre-multiplied power spectrum (left) of streamwise velocity fluctuations for the forced flow and the difference spectrum (right) between the forced and canonical flows at station-1 ($x = 2.7\delta$). The difference spectrum shows the fractional change in power levels in presence of the synthetic mode $\left(E_{uu}^F - E_{uu}^C\right)$ relative to the canonical flow $\left(E_{uu}^C\right)$. In both plots the vertical line at $\lambda_\gamma = 5\delta$ indicates the scale filter cut-off location, and the horizontal dashed line at $y_c = 0.072\delta$ indicates the estimated critical layer location for the synthetic mode.

be reduced to the form

$$S = \frac{6}{4\sigma^3} \sum_{\substack{\forall\, l,m,n \,| \\ k_l<k_m<k_n \\ k_l+k_m=k_n}} \alpha_l \alpha_m \alpha_n \sin(\phi_l + \phi_m - \phi_n) + \frac{3}{4\sigma^3} \sum_{\substack{l=1 \\ (k_n=2k_l)}}^{\infty} \alpha_l^2 \alpha_n \sin(2\phi_l - \phi_n). \quad (2)$$

From the above equation it is seen that skewness is nothing but a weighted (by mode amplitudes) and normalized (by σ^3) sum of the quantity $\sin(\phi_l + \phi_m - \phi_n)$ over all sets of triads $\{k_l, k_m, k_n\}$ and wavenumber pairs $\{k_l, k_n\}$ such that $k_l = k_n - k_m$ and $2k_l = k_n$ respectively.

We now consider the amplitude modulation coefficient R following the procedure outlined by Mathis *et al.* (2009). The velocity signal is split into large- and small-scale components using a spatial Fourier filter a set wavenumber k_γ

$$u_L = \sum_{i=1}^{\gamma-1} \alpha_i \sin(k_i x + \phi_i), \quad u_S = \sum_{i=\gamma}^{\infty} \alpha_i \sin(k_i x + \phi_i). \quad (3)$$

Note that for $\lambda_\gamma = 2\pi/k_\gamma$ is set at 5δ for experimental data analysis. An envelope $\mathscr{E}$ of the small-scale signal is obtained using a Hilbert transform procedure (see DM15 for details), and R is defined to be the correlation coefficient between the large-scale signal and the large-scale component of $\mathscr{E}$, written as $\mathscr{E}_L$. From equation 3, the expression for R can be reduced to the form

$$R = \frac{\langle u_L \mathscr{E}_L \rangle}{\langle u_L^2 \rangle^{\frac{1}{2}} \langle \mathscr{E}_L^2 \rangle^{\frac{1}{2}}} = \frac{1}{\Omega} \sum_{\substack{\forall\, l,m,n \,| \\ k_n-k_m=k_l \\ 0<k_l<k_\gamma \\ k_m,k_n>k_\gamma}} \alpha_l \alpha_m \alpha_n \sin(\phi_l + \phi_m - \phi_n), \quad (4)$$

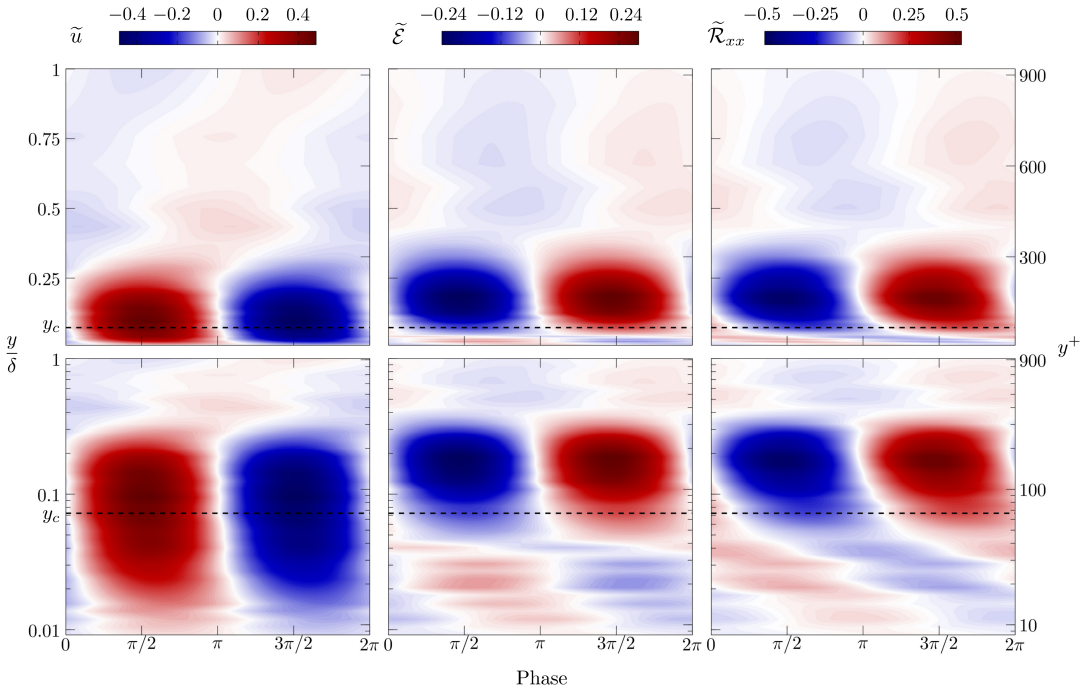

Figure 3. Synthetic mode $\widetilde{u}$ (left), triadic small-scale envelope $\widetilde{\mathscr{E}}$ (center), and Reynolds stress component $\widetilde{\mathscr{R}}_{xx}$ (right) over one temporal period at station-1. The top and bottom panels are scaled linearly and logarithmically respectively in y. Data in this figure are in raw units, ms^{-1} for $\widetilde{u}$, and $\mathrm{m}^2\mathrm{s}^{-2}$ for $\widetilde{\mathscr{E}}$ and $\widetilde{\mathscr{R}}_{xx}$.

where $\Omega = \langle u_L^2\rangle^{\frac{1}{2}}\langle \mathscr{E}_L^2\rangle^{\frac{1}{2}}$ is the normalization factor for the covariance $\langle u_L \mathscr{E}_L\rangle$. Only triadic wavenumbers contribute to R in a manner similar to S. However, the filtering process places a restriction on the class of triadic sets $\{k_l, k_m, k_n\}$; assuming without a loss of generality that $k_l < k_m < k_n$, the large scale k_l and the small scales k_m, k_n necessarily lie on either side of the filter cut-off k_γ to make a non-zero contribution R.

Following the phase interpretation of Chung & McKeon (2010), it is seen that $\phi_l + \phi_m - \phi_n = \Delta\phi$ in equation 4 is the phase difference (with a $\pi/2$ radians offset) between the large-scale k_l and the envelope of the triadic small-scales k_m, k_n. Hence R can be interpreted as an amplitude-weighted (and normalized) phase measure $\sin(\Delta\phi)$ of all large- and small-scale triadic interactions. Notice that skewness (equation 2) is also a measure of the same phase quantity, but over all triadic interactions with no scale restrictions. By considering the quantities $\langle u_S^3\rangle, \langle u_L^3\rangle, \langle u_L^2 u_S\rangle$ in a manner similar to $\langle u^3\rangle$ and $\langle u_L \mathscr{E}_L\rangle$, the following exact relationship between S and R can be written (see DM15 for details)

$$\sigma^3 S \;=\; 1.5\,\Omega R + \langle u_S^3\rangle + \langle u_L^3\rangle + 3\langle u_L^2 u_S\rangle. \qquad (5)$$

The influence of the synthetic large scale on the naturally existing triadic phase relationship can be seen in changes to values of S and R. Figure 4 shows the difference ΔS and ΔR between the forced and canonical flows in the wall-normal region around the critical layer. There is a marked increase in the values of S and R in the region $0.02\delta < y < 0.1\delta$ and decrease in the region $0.1\delta < y < 0.4\delta$ in presence of the synthetic large-scale. The cross-over location $y/\delta = 0.1$ corresponds well to the synthetic mode peak location (see figure 5), and is close to the estimated

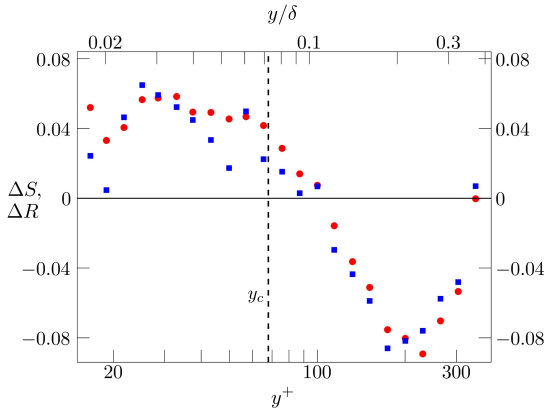

Figure 4. Changes in the skewness $\Delta S = S^F - S^C$ (•) and the amplitude modulation coefficient $\Delta R = R^F - R^C$ (▪) in presence of the synthetic large scale.

critical layer location. The results in figure 4 suggest that the synthetic large-scale drives the envelope of all small-scales towards being in ($\Delta S, \Delta R > 0$) and out ($\Delta S, \Delta R < 0$) of phase with it below and above its critical layer location respectively, thereby altering the natural large- and small-scale phase relationships (or the degree of amplitude modulation) in the flow.

SMALL-SCALE ORGANIZATION

The direct influence of the synthetic large-scale is seen on the small-scales that couple in a triadic manner. Consider two small-scale triadic wavenumbers k_m, k_n ($> k_\gamma$) that couple directly to the synthetic large-scale, *i.e.* $k_n - k_m = k_{sls}$;

the envelope of k_m, k_n has a wavenumber of k_{sls} due to the triadic condition. An average triadic envelope of all such small-scale wavenumbers k_m, k_n can be obtained in the following simple manner. The small-scale velocity u_S (equation 3) is squared (u_S^2) then phase-averaged with respect to the forcing signal and mean removed (denoted by $\widetilde{u_S^2} - \langle \widetilde{u_S^2} \rangle = \widetilde{\mathscr{E}}$). The phase-averaging procedure picks out the component corresponding to k_{sls} from u_S^2,

$$\widetilde{\mathscr{E}} = \sum_{\substack{\forall m,n \mid \\ k_n - k_m = k_{sls} \\ k_m, k_n > k_\gamma}} \frac{1}{2} \alpha_m \alpha_n \cos(k_{sls} x + \phi_n - \phi_m). \qquad (6)$$

For a specific set of small-scale triadic wavenumbers k_m, k_n such that $u_{mn} = \alpha_m \sin(k_m x + \phi_m) + \alpha_n \sin(k_n x + \phi_n)$, an envelope $A(x)$ can be written as the square of the analytic function modulus following DM2015, *i.e.* $A(x) = u_{mn}^2(x) + \mathscr{H}^2(x)$, where $\mathscr{H}$ is the Hilbert transform of u_{mn}. After removing the mean terms A reduces to the following form

$$\begin{aligned} A(x) &= 2\alpha_m \alpha_n \cos[(k_n - k_m)x + \phi_n - \phi_m] \\ &= 2\alpha_m \alpha_n \cos(k_{sls} x + \phi_n - \phi_m). \end{aligned} \qquad (7)$$

A straightforward comparison between equations 6 and 7 reveals that, in essence, $\widetilde{\mathscr{E}}$ captures the amplitude-weighted average phase of the triadic envelope across all sets of small-scale wavenumbers that couple directly with the synthetic scale.

The center panels in figure 3 show $\widetilde{\mathscr{E}}$ from the experiment. A certain correlation between the synthetic large scale ($\widetilde{u}$) and the average small-scale triadic envelope ($\widetilde{\mathscr{E}}$) can be seen by just a visual inspection of the figure. The two quantities are in phase close to the wall, and out of phase away from it following an abrupt jump of π radians in the phase of $\widetilde{\mathscr{E}}$ close to the critical layer location. The phase relationship can be analyzed in a quantitative manner by defining a correlation coefficient Ψ between $\widetilde{u}$ and $\widetilde{\mathscr{E}}$, akin to the amplitude modulation coefficient R

$$\Psi = \frac{\left\langle \widetilde{u}\, \widetilde{\mathscr{E}} \right\rangle}{\left\langle \widetilde{u}^2 \right\rangle^{1/2} \left\langle \widetilde{\mathscr{E}}^2 \right\rangle^{1/2}} . \qquad (8)$$

Note that R gives the average phase between all large- and small-scales in the flow (including the synthetic scale when present), whereas Ψ is a measure of the phase between the synthetic scale and the average triadic envelope of small-scales that are in direct coupling. Thus Ψ represents the coupling due to one wavenumber within the broader u_L. $\Psi(y)$ at station-1 is shown in figure 5 along with the normalized energy of the synthetic large-scale. The wall-normal locations where the synthetic large-scale energy drops to 15% of its peak value are shown by dash-dot lines for reference; the region between these lines is where effects of the synthetic large-scale are expected to dominate. As the energy in the synthetic mode drops close to zero, the correlation coefficient Ψ becomes noisy (outside the 15% energy reference lines). A clear organization in phase of directly coupled small-scales by the synthetic large-scale is seen in the region where the synthetic scale is active. The triadic small-scales are in phase with the synthetic large-scale ($\Psi = 1$) near the wall and out of phase ($\Psi = -1$) away from the wall; a sharp phase jump of π radians occurs at $y = 0.04\delta$, close to the estimated critical layer location. The phase behavior of the directly coupled small-scales is consistent with the altered large and small-scale phase relationship suggested by skewness and amplitude modulation coefficient.

The quantity $\widetilde{\mathscr{E}}$ can also be interpreted in a more traditional manner in terms of the normal streamwise component $\mathscr{R}_{xx}$ $\left(\equiv \langle u^2 \rangle\right)$ of the Reynolds stress tensor $\mathscr{R}$. The oscillatory component of $\mathscr{R}_{xx}$ due to the forcing (denoted by $\widetilde{\mathscr{R}}_{xx}$) can be obtained by the phase-averaging procedure described earlier; we write $\widetilde{\mathscr{R}}_{xx} = \widetilde{u^2} - \langle \widetilde{u^2} \rangle$. Although $\widetilde{\mathscr{E}}$ and $\widetilde{\mathscr{R}}_{xx}$ are similar quantities, the scale restriction imposed on the velocity fluctuations in the calculation of $\widetilde{\mathscr{E}}$ means that it represents only the contributions from small-scale velocity fluctuations to the oscillating Reynolds stress.

The phase variation of $\widetilde{\mathscr{R}}_{xx}(y)$, seen in figure 3 (right panel), is very similar to that of $\widetilde{\mathscr{E}}(y)$. The phase relationship between synthetic large scale and the oscillating Reynolds stress can be quantified in terms of correlation coefficient Φ (similar to Ψ)

$$\Phi = \frac{\left\langle \widetilde{u}\, \widetilde{\mathscr{R}}_{xx} \right\rangle}{\left\langle \widetilde{u}^2 \right\rangle^{1/2} \left\langle \widetilde{\mathscr{R}}_{xx}^2 \right\rangle^{1/2}} . \qquad (9)$$

As expected from a visual inspection of figure 3, a phase jump of π radians between $\widetilde{u}$ and $\widetilde{\mathscr{R}}_{xx}$ is seen from the behavior of Φ near the critical layer. This phase jump can be predicted from a simplified transfer function formulation between the isolated synthetic scale and the oscillatory Reynolds stress obtained from the governing Navier-Stokes equations, this is a subject of ongoing research (Chung *et al.*, in preparation). The role of the critical layer in anchoring the wall-normal location of phase reversal between large and small scales, *i.e.* the zero-crossing locations of R and Ψ is also under investigation.

CONCLUDING REMARKS

The natural triadic phase relationships in a turbulent boundary were manipulated by synthetically introducing a large-scale motion in the flow. By interpreting the skewness and the amplitude modulation coefficient of the streamwise velocity signal as a measure of the average phase in triadically consistent wavenumber interactions, the synthetic large scale is shown to alter such phase relationships in a quasi-deterministic manner. Note that the phase relationships are discussed here in a time-averaged sense, the instantaneous flow field is still *turbulent*, and hence the term quasi-deterministic. The influence of the synthetic large-scale on directly coupled small scales is understood by defining an average triadic small-scale envelope $\widetilde{\mathscr{E}}$; a clear phase-locking or organization effect is seen on the small scales. The quantity $\widetilde{\mathscr{E}}$ is related to the traditionally studied normal streamwise component of the oscillatory Reynolds stress $\widetilde{\mathscr{R}}_{xx}$. Efforts are presently being made to model the observed phase relationships between the isolated synthetic scale and the Reynolds stress directly from the Navier-Stokes equations, and also understand the role of the critical layer in the same context.

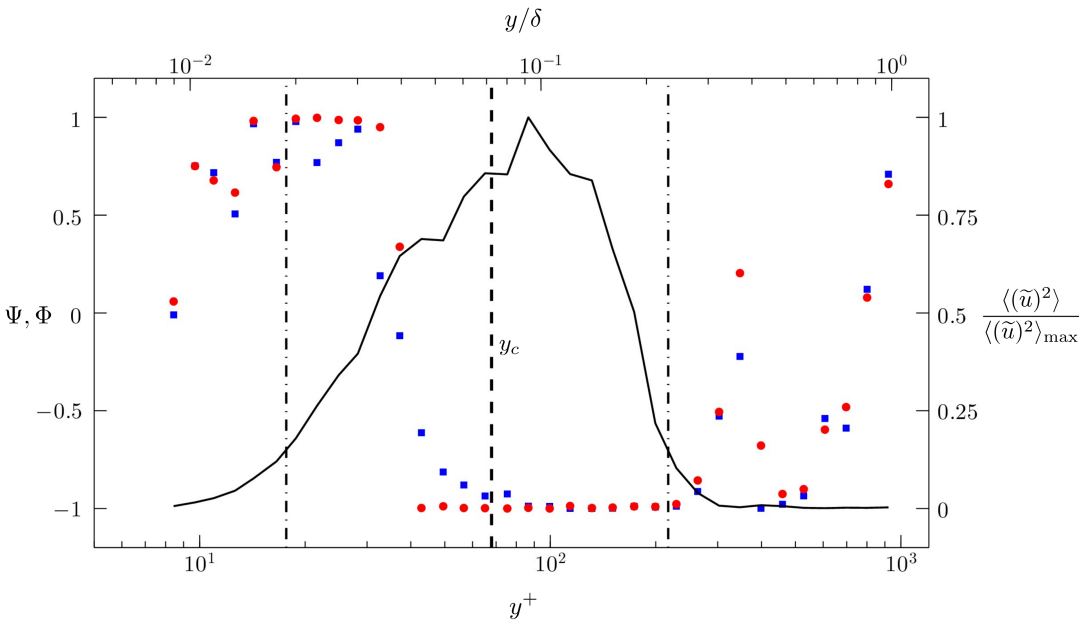

Figure 5. Correlation coefficients Ψ (•), Φ (▪), and normalized synthetic mode energy (–). The estimated critical layer location y_c is marked by a dashed line, and the locations where the synthetic mode energy drops to 15% of it's peak value are marked by dash-dot lines.

The experimental technique presented here helps us better understand the scale coupling in turbulent wall-bounded flows through deterministic perturbations. In conjunction with the resolvent based model of the Navier-Stokes equations (*e.g.* Sharma & McKeon, 2013), the results presented here open the possibility of setting up a practical framework for favorable manipulation of energetic near-wall small-scale turbulence through large-scale inputs.

The authors gratefully acknowledge AFOSR (grant FA 9550-12-1-0469, program manager D. Smith) for the financial support of this work, and a graduate fellowship (SD) from the Resnick Institute at Caltech.

REFERENCES

Bandyopadhyay, P. R. & Hussain, A. K. M. F. 1984 The coupling between scales in shear flows. *Physics of Fluids* **27** (9), 2221–2228.

Bernardini, M. & Pirozzoli, S. 2011 Inner/outer layer interactions in turbulent boundary layers: A refined measure for the large-scale amplitude modulation mechanism. *Physics of Fluids* **23** (6), 061701.

Brown, G. L. & Thomas, A. S. W. 1977 Large structure in a turbulent boundary layer. *Physics of Fluids* **20** (10), S243–S252.

Chung, D., Duvvuri, S., Jacobi, I. & McKeon, B. J. (in preparation) Interactions between scales in wall turbulence: phase relationships, amplitude modulation and the importance of critical layers.

Chung, D. & McKeon, B. J. 2010 Large-eddy simulation of large-scale structures in long channel flow. *Journal of Fluid Mechanics* **661**, 341–364.

Duvvuri, S. & McKeon, B. J. 2014 Phase relationships in presence of a synthetic large-scale in a turbulent boundary layer. In *44th AIAA Fluid Dynamics Conference, Atlanta GA, June 2014*. AIAA paper 2014-2883.

Duvvuri, S. & McKeon, B. J. 2015 Triadic scale interactions in a turbulent boundary layer. *Journal of Fluid Mechanics* **767**, R4.

Hussain, A. K. M. F. & Reynolds, W. C. 1970 The mechanics of an organized wave in turbulent shear flow. *Journal of Fluid Mechanics* **41**, 241–258.

Hutchins, N. & Marusic, I. 2007 Large-scale influences in near-wall turbulence. *Philosophical Transactions of the Royal Society A* **365**, 647–664.

Jacobi, I. & McKeon, B. J. 2011 Dynamic roughness perturbation of a turbulent boundary layer. *Journal of Fluid Mechanics* **688**, 258–296.

Jacobi, I. & McKeon, B. J. 2013 Phase relationships between large and small scales in the turbulent boundary layer. *Experiments in Fluids* **54** (3), 1481.

Mathis, R., Hutchins, N. & Marusic, I. 2009 Large-scale amplitude modulation of the small-scale structures in turbulent boundary layers. *Journal of Fluid Mechanics* **628**, 311–337.

Mathis, R., Marusic, I., Hutchins, N. & Sreenivasan, K. R. 2011 The relationship between the velocity skewness and the amplitude modulation of the small scale by the large scale in turbulent boundary layers. *Physics of Fluids* **23** (12), 121702.

Rao, K. N., Narasimha, R. & Narayanan, M. A. B. 1971 The 'bursting' phenomenon in a turbulent boundary layer. *Journal of Fluid Mechanics* **48**, 339–352.

Schlatter, P. & Örlu, R. 2010 Quantifying the interaction between large and small scales in wall-bounded turbulent flows: A note of caution. *Physics of Fluids* **22** (5), 051704.

Sharma, A. S. & McKeon, B. J. 2013 On coherent structure in wall turbulence. *Journal of Fluid Mechanics* **728**, 196–238.

Smits, A. J., McKeon, B. J. & Marusic, I. 2011 High-Reynolds number wall turbulence. *Annual Review of Fluid Mechanics* **43**, 353–375.